Coupled-resonator-induced transparency

David D. Smith,[1,2] Hongrok Chang,[1,2] Kirk A. Fuller,[1,3] A. T. Rosenberger,[4] and Robert W. Boyd[5]
[1]*Science Directorate, NASA Marshall Space Flight Center, Huntsville, Alabama 35812, USA*
[2]*Department of Physics, University of Alabama in Huntsville, Huntsville, Alabama 35899, USA*
[3]*Earth Science Systems Group, National Space Science and Technology Center, Department of Atmospheric Sciences, University of Alabama in Huntsville, Huntsville, Alabama 35899, USA*
[4]*Department of Physics, Oklahoma State University, Stillwater, Oklahoma 74078, USA*
[5]*Institute of Optics, University of Rochester, Rochester, New York 14627, USA*
(Received 22 September 2003; published 3 June 2004)

We demonstrate that a cancellation of absorption occurs on resonance for two (or any even number of) coupled optical resonators, due to mode splitting and classical destructive interference, particularly when the resonator finesse is large and the loss in the resonator farthest from the excitation waveguide is small. The linewidth and group velocity of a collection of such coupled-resonator structures may be decreased by using larger resonators of equal size, by using larger resonators of unequal size where the optical path length of the larger resonator is an integer multiple of that of the smaller one, or by using a larger number of resonators per structure. We explore the analogy between these effects and electromagnetically-induced transparency in an atomic system.

DOI: 10.1103/PhysRevA.69.063804 PACS number(s): 42.60.Da, 42.50.Gy, 42.55.Sa, 32.80.−t

Electromagnetically-induced transparency (EIT) is a phenomenon that can occur in atomic systems as a result of the destructive interference between excitation pathways to the upper level. This interference occurs in single atoms but manifests itself at the macroscopic level. Naturally, one is led to ask whether EIT-like effects can occur through classical means. Recently, classical interference of fields (rather than probability amplitudes) due to collective electronic effects has been proposed for propagation at frequencies below the cutoff frequency of an ideal plasma [1], as well as at the electron-cyclotron resonance of a cold plasma [2]. Classical analogs of EIT can also be demonstrated in systems of mechanical or electrical oscillators, where the destructive interference between in-phase and out-of-phase normal modes results in no power transfer to the system even when a probe excitation is present [3–5].

Similarly, in this paper we demonstrate that EIT-like effects can be established in coupled optical resonators due to classical destructive interference. Yariv *et al.* have shown that extensive mode splitting occurs in coupled-resonator optical waveguides (CROW's), leading to the formation of photonic bands [6]. In addition, we have found that whispering gallery modes (WGM's) in coupled microresonators are split symmetrically when the individual resonators have the same optical path length (OPL), due to the fact that light must traverse a coupler twice, acquiring a net π phase shift before interfering with light in the initial resonator [7]. Notably, in contrast to EIT where the Autler-Townes splitting arises from the ac Stark effect induced by an auxiliary external field [8], the splitting in coupled (mechanical, electrical, or, as in the case examined here, optical) resonators is the result of an internal coupling between individual oscillators. For this reason, coupled-resonator-induced transparency (CRIT) does not suffer from the propagation scaling limitations of EIT as a result of control field absorption.

To elucidate the analogy between atomic and photonic coherence effects, let us first briefly review EIT in an atomic three-level Λ configuration as shown in Fig. 1. The $|1\rangle$-$|3\rangle$ transition is assumed to be dipole disallowed. When a strong control field is resonantly applied to the $|3\rangle$-$|2\rangle$ transition, the excited state $|2\rangle$ splits into the dressed states $|\pm\rangle = (|2\rangle \mp |3\rangle)/\sqrt{2}$, separated by the Rabi frequency of the control (or coupling) field Ω_c. The absorption of a weak probe beam ($\Omega_p \ll \Omega_c$), resonant with the $|1\rangle$-$|2\rangle$ transition, vanishes either (i) when the Rabi frequency of the control field is larger than the excited-state lifetime-broadened linewidth ($\Omega_c > \Gamma$, where $\Gamma = \Gamma_{21} + \Gamma_{23}$) or (ii) when the splitting is smaller than the linewidth ($\Omega_c < \Gamma$) but Fano-type interference [9] occurs between the two indistinguishable quantum-mechanical paths. The interference is destructive owing to a π-phase difference between the two contributions to the atomic response at the probe frequency. For the case of zero detuning of the control field and a decay rate of zero for the $|1\rangle$-$|3\rangle$ transition ($\Gamma_{31} = \Gamma_{13} = 0$), the transition rate for the absorption of an arbitrarily detuned probe beam is given by [10]

$$W(\Delta) = \frac{[\Omega_p^2/\Gamma]}{1 + \frac{4}{\Gamma^2}\left[\Delta - \frac{(\Omega_c/2)^2}{\Delta}\right]^2} = [\Omega_p^2/\Gamma]K, \qquad (1)$$

where Ω_p and Δ are the Rabi frequency and angular frequency detuning of the probe field, respectively, and Γ is the decay rate from level $|2\rangle$ to levels $|1\rangle$ and $|3\rangle$. Equation (1) is the expression for a split Lorentzian. When $\Omega_c \to 0$ this expression reduces to that of a single Lorentzian with a full width at half maximum (FWHM) of Γ. The corresponding atomic absorption cross section is $\sigma(\Delta) = \sigma_0 K = [\hbar\omega/I]W = \alpha/\rho$ where $\sigma_0 = [\Omega_p^2/\Gamma]\hbar\omega/I$ is the maximum cross section (line center when $\Omega_c \to 0$), $K(\Delta)$ is the dimensionless cross section or line-shape function, α is the absorption coefficient, ρ is the number density of (dressed) atoms, and ω and I are

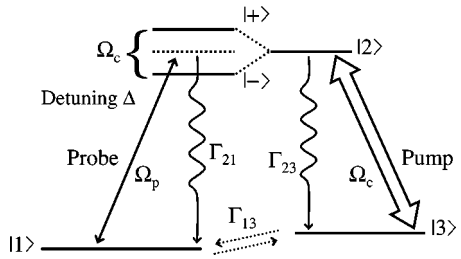

FIG. 1. Typical energy level diagram for the observation of EIT.

the angular frequency and intensity of the probe, respectively [11].

Next we consider the unidirectional propagation and partial coupling of light from a straight waveguide into N ring resonators coupled together as shown in Fig. 2. Taking an iterative approach [7], one readily finds that the absorptance of light due to rings 1 through j is given by

$$\tilde{A}_j(\phi_j,\phi_{j-1},\ldots,\phi_1) \equiv 1-\tilde{T}_j = \frac{\tilde{A}_j^{(\mathrm{env})}}{1+\tilde{F}_j \sin^2\left(\dfrac{\tilde{\phi}_{j-1}^{(\mathrm{eff})}+\phi_j}{2}\right)}, \tag{2}$$

where

$$\tilde{A}_j^{(\mathrm{env})}(\phi_{j-1},\phi_{j-2},\ldots,\phi_1) \equiv \frac{(1-r_j^2)(1-a_j^2|\tilde{\tau}_{j-1}|^2)}{[1-r_j a_j|\tilde{\tau}_{j-1}|]^2} \tag{3}$$

is an envelope function,

$$\tilde{F}_j(\phi_{j-1},\phi_{j-2},\ldots,\phi_1) \equiv \frac{4r_j a_j|\tilde{\tau}_{j-1}|}{[1-r_j a_j|\tilde{\tau}_{j-1}|]^2} \tag{4}$$

is a function related to finesse, r_j and $t_j=\sqrt{1-r_j^2}$ are the reflection and transmission coefficients of the jth coupler, respectively, $\phi_j=\beta_j L_j$ and $a_j=e^{-\alpha_j L_j/2}$ are the single-pass phase shift and attenuation factor for the jth ring, respectively, and α_j, L_j, and β_j are the absorption coefficient, length, and propagation constant of the jth ring, respectively. The factors

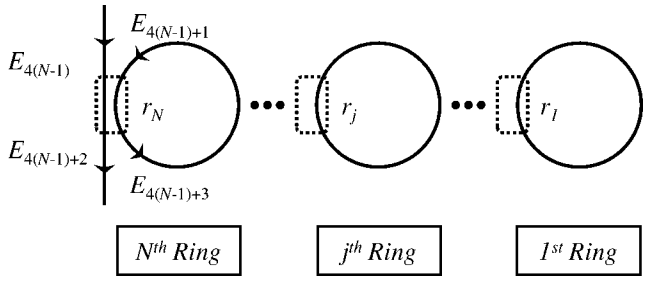

FIG. 2. Illustration of N coupled ring resonators. The numbering scheme for the rings and electric fields is shown.

$$\tilde{\tau}_j(\phi_j,\phi_{j-1},\ldots,\phi_1) \equiv \frac{\tilde{E}_{4(j-1)+2}}{\tilde{E}_{4(j-1)}} = \frac{r_j - a_j\tilde{\tau}_{j-1}e^{i\phi_j}}{1-r_j a_j\tilde{\tau}_{j-1}e^{i\phi_j}} \tag{5}$$

and

$$\tilde{\phi}_j^{(\mathrm{eff})}(\phi_j,\phi_{j-1},\ldots,\phi_1) \equiv \arg(\tilde{\tau}_j) = \pi+\phi_j + \arg\left(\frac{a_j\tilde{\tau}_{j-1}-r_j e^{-i\phi_j}}{1-r_j a_j\tilde{\tau}_{j-1}e^{i\phi_j}}\right) \tag{6}$$

represent the complex transmission coefficient and effective phase shift for the jth ring, respectively, where $\tau_0=1$ and $\phi_0^{(\mathrm{eff})}=0$. The transmittance across the jth ring is simply $\tilde{T}_j=|\tilde{\tau}_j|^2$. For compactness, quantities that depend on single-pass phase shifts are denoted by a tilde, with explicit dependences only included on the left-hand side of the expressions.

For a single ring $A_1^{(\mathrm{env})}$ and F_1 are simply coefficients, independent of the single-pass phase shift. Equation (2) then becomes the typical Airy profile, having a *maximum* value of $A_1^{(\mathrm{env})}$ at resonance ($\phi_1 \bmod 2\pi=0$), a minimum value of $A_1^{(\mathrm{env})}/(1+F_1)$ at antiresonance ($\phi_1 \bmod 2\pi=\pi$), and a width inversely related to the coefficient of finesse F_1. Thus, for large F_1, the small-angle approximation is valid over the entire resonance—i.e., $\sin(\phi_1/2)\approx(\phi_1/2)$—and the resonant features are well approximated by Lorentzians each having a FWHM of $4/\sqrt{F_1}$. For two rings the situation is much different. In this case Eq. (2) becomes

$$\tilde{A}_2(\phi_2,\phi_1) = \frac{\tilde{A}_2^{(\mathrm{env})}}{1+\tilde{F}_2 \sin^2\left(\dfrac{\tilde{\phi}_1^{(\mathrm{eff})}+\phi_2}{2}\right)}. \tag{7}$$

When the OPL's of the two rings are identical, such that $\phi_1=\phi_2=\phi$ (analogous to a degenerate atomic Λ system), this equation displays a *minimum* at the single-ring resonances ($\phi \bmod 2\pi=0$), resulting in a splitting, as shown in Fig. 3(a), where A_2 is plotted for $a_1=0.9999$, $a_2=0.88$, $r_1=0.999$, and $r_2=0.9$.

The analogy with EIT is made clearer by assuming $a_1=1$ (analogous to the assumption $\Gamma_{31}=\Gamma_{13}=0$). $A_2^{(\mathrm{env})}$ and F_2 are then independent of the single-pass phase shifts (because $|\tilde{\tau}_1|=1$), and Eq. (7) becomes directly analogous to Eq. (1). Again, in contrast with a single ring, Eq. (7) displays a minimum value of $A_2^{(\mathrm{env})}/(1+F_2)$ at the single-ring resonances ($\phi \bmod 2\pi=0$) and antiresonances ($\phi \bmod 2\pi=\pi$) and a maximum value of $A_2^{(\mathrm{env})}$ at $(\phi_1^{\mathrm{eff}}+\phi_2)\bmod 2\pi=0$,—i.e., between resonance and antiresonance. Note that when $t_1\to 0$ (analogous to $\Omega_c\to 0$), $\tilde{\phi}_1^{(\mathrm{eff})}\to 0$ and Eq. (7) reduces to the typical Airy profile for a single (uncoupled) ring. However, for $t_1>0$ a splitting occurs because $\tilde{\phi}_1^{(\mathrm{eff})}=\pi$ at the single-ring resonance, which leads to a minimum in the absorption. The phase difference between the split modes increases with t_1 according to $\Delta\phi=2\sin^{-1}(t_1)$, taking its maximum value $\Delta\phi^{(\max)}=\pi$ (half the free spectral range) when $t_1\to 1$, at which point the spectrum simply becomes identical to that of

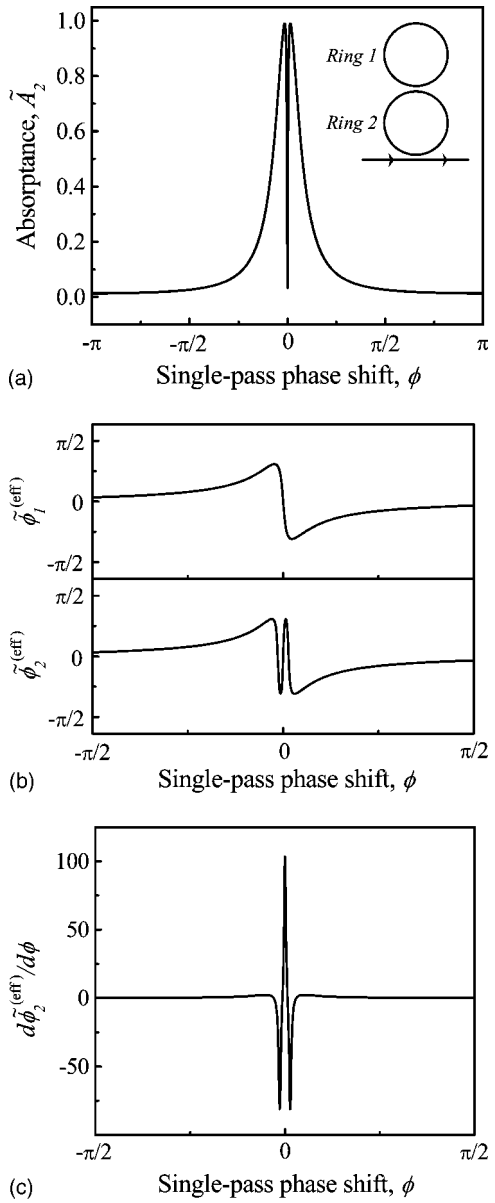

FIG. 3. (a) Absorptance vs single-pass phase shift for two coupled ring resonators with $a_1=0.9999$, $a_2=0.88$, $r_1=0.999$, and $r_2=0.9$. The resonance is split, analogous to the Autler-Townes splitting and destructive interference that occurs in three-level atomic systems, such that transparency rather than absorption occurs for $\phi_1=\phi_2=0$. (b) Effective phase shift for a single ring resonator ($\phi_1^{(\mathrm{eff})}$) and for two coupled ring resonators ($\phi_2^{(\mathrm{eff})}$). Whereas anomalous dispersion occurs on resonance for (a), normal dispersion occurs for (b). (c) The slope of the effective phase shift vs the single-pass phase shift for two coupled rings. This quantity is proportional to the difference between the group index and the phase index. The light is slowed by a factor of about $100\rho Z$ on resonance.

a ring with twice the optical path length of the individual rings. In this strong-coupling limit, interference between the normal modes of the structure has no significant effect on the resonant features. The absorption at the single-ring resonance is minimized simply because the splitting is so large. In the weak-coupling limit, on the other hand, the modes become close together and, if not for interference, their independent overlap would result in significant absorption. In this limit, therefore, it is the interference of light circulating in one ring with that in the adjacent ring that leads to induced transparency.

Hence, the transmission coefficient of the first coupler, t_1, is analogous to the coupling Rabi frequency Ω_c and determines the spacing between the split modes—i.e., the CRIT linewidth. In addition, the phase mismatch between the incident light and the single-ring resonance frequencies ϕ_2 models the probe field detuning Δ, while the coupler transmission t_2 corresponds to the probe Rabi frequency Ω_p. The attenuation factor a_1 models Γ_{13}, the rate of nonradiative population transfer between the ground states $|1\rangle$ and $|3\rangle$, while a_2 models the decay rate Γ from the upper level (primarily spontaneous emission). The destructive interference in CRIT results from the $\pi/2$ phase shift that occurs when light crosses a coupler. Two passes across a coupler are required, and hence a π-phase shift, for light in adjoining rings to interfere. Comparison of Eqs. (1) and (7), however, reveals an important difference between CRIT and EIT. CRIT involves split Airy expressions, whereas EIT involves split Lorentzians. This distinction is negligible when the resonator finesse is sufficiently large, but presents a limitation on the induced transparency as the finesse decreases because, unlike a Lorentzian, an Airy profile is periodic and so does not asymptotically approach zero. In both cases the transparency is limited to that experienced at antiresonance, but this is lower in CRIT due to the periodicity of the Airy profile. In the limits where CRIT can be described by a split Lorentzian, the analogies between EIT and CRIT quantities can be made more definite. For two resonators with identical OPL's, under the assumption that $a_1=1$, Eq. (6) can be rewritten as $\sin^2[(\tilde{\phi}_1^{(\mathrm{eff})}+\phi_2)/2]=(r_1-\cos\,\phi_2)^2/(1+r_1^2-2r_1\cos\,\phi_2)$. For small detunings $\cos\,\phi_2\approx 1-(\phi_2^2/2)$, and for sufficiently weak coupling between resonators $(1-r_1)^2\ll r_1\phi_2^2$. Substituting these results into Eq. (7) and transforming to angular frequencies yields a split Lorentzian

$$\tilde{A}_2(\delta)=\frac{A_2^{(\mathrm{env})}}{1+\dfrac{4}{\gamma^2}\left[\delta-\dfrac{(\Delta\omega/2)^2}{\delta}\right]^2}=A_2^{(\mathrm{env})}\kappa, \tag{8}$$

where $\gamma=1/\tau_D=4\sqrt{(r_1/F_2)}/\tau_R=2(1-r_2a_2)/\sqrt{\eta}\tau_R$ is related to the linewidth, $\eta=r_2a_2/r_1$, τ_D is reminiscent of the photon decay time (analogous to the lifetime of state $|2\rangle$), τ_R is the single-ring round-trip time, $\Delta\omega=\Delta\phi/\tau_R=2\sqrt{2(1-r_1)}/\tau_R$ is the frequency difference between the split modes, and $\delta=\phi_2/\tau_R$ is the detuning. Note that Eq. (8) is formally identical to Eq. (1) and accurately describes CRIT for phase detunings $(1-r_1)/\sqrt{r_1}\ll\phi_2\ll 1$. Hence, in these limits, the analogies between CRIT and EIT are $\Delta\rightarrow\delta$, $\Gamma\rightarrow\gamma$, $\Omega_c\rightarrow\Delta\omega$, and $K(\Delta)\rightarrow\kappa(\delta)$ for the quantities in the denominators. Because the incident power in the waveguide P, linear number density of structures λ, and absorptance $\tilde{A}_2(\delta)$ play roles in CRIT similar to those played by the probe intensity I, volume density of atoms ρ, and cross section $\sigma(\Delta)$ in EIT, respectively, we find the additional analogy Ω_p

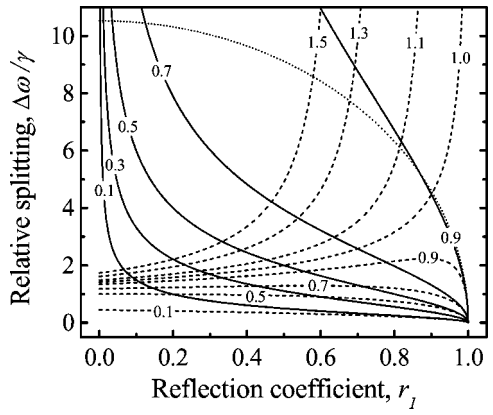

FIG. 4. Relative splitting $\Delta\omega/\gamma$ plotted vs r_1 for various values of r_2a_2 (solid curve) and η (dashed curve). The dotted curve represents the approximation of small resonator losses for $r_2a_2=0.9$.

$\rightarrow 2t_2\sqrt{(1-a_2^2)(P/\eta\gamma\hbar\omega)}/\tau_R$, for the quantities in the numerators. Note that in the limit of small resonator losses $a_2^2 \approx 1-\alpha_2 L_2$ and $\eta \approx 1-(t_2^2+\alpha_2 L_2-t_1^2)/2 \approx 1$, which yields $\Omega_p \approx 2t_2\sqrt{(\alpha_2 L_2 P/\gamma\hbar\omega)}/\tau_R$ and $\gamma \approx (t_2^2+\alpha_2 L_2)/\tau_R \approx \gamma_2$—i.e., γ is simply related to the total (coupling and internal) loss rate of the resonator coupled to the excitation waveguide, γ_2. In this limit $\Delta\omega \approx 2t_1/\tau_R$ is also obtained, which reminds us of the main physical point, that the coupling between resonators t_1 is responsible for the mode splitting, in analogy with the Rabi frequency of the control field Ω_c.

Unlike the EIT variables Γ and Ω_c, the corresponding CRIT variables γ and $\Delta\omega$ are only independent in the limit of small resonator losses. The independent variables r_1 and r_2a_2 determine the character of the transparency through the relative splitting

$$\frac{\Delta\omega}{\gamma} = \frac{\sqrt{2\eta(1-r_1)}}{1-r_2a_2}, \tag{9}$$

plotted in Fig. 4. This parameter specifies the extent to which the resonators can be considered to be independent (distinguishable). In particular, when $\Delta\omega/\gamma \geqslant 1$ the response can be approximated as the sum of two distinct Lorentzians [10] at $\delta=\pm\Delta\omega/2$—i.e., $\kappa(\delta) \approx \kappa_+ + \kappa_-$ where $\kappa_+(\delta)=1/\{1+[4(\delta-\Delta\omega/2)/\gamma]^2\}$ and $\kappa_-(\delta)=1/\{1+[4(\delta+\Delta\omega/2)/\gamma]^2\}$. The two Lorentzians $\kappa_+(\delta)$ and $\kappa_-(\delta)$ are just resolved when $\Delta\omega/\gamma=1$—i.e., when $r_1=2r_2a_2/[1+(r_2a_2)^2]$. Hence, the regime $\Delta\omega/\gamma \geqslant 1$ is analogous to EIT for distinguishable upper states $|\pm\rangle$—i.e., for $\Omega_c > \Gamma$, where transparency results primarily from the ac Stark effect. In contrast, for $\Delta\omega/\gamma < 1$ the interference due to coupling between the normal modes of the structure cannot be neglected, and the associated strong dispersion results in light that is considerably slowed. Utilizing the relationships $\gamma \approx \gamma_2$ and $\Delta\omega \approx 2\sqrt{\gamma_1/\tau_R}$, valid for small resonator losses, and recognizing that $1/\tau_R \gg \gamma_1$ for high-Q resonators, Eq. (9) becomes

$$\frac{\Delta\omega}{\gamma} \approx \frac{2t_1}{t_2^2+\alpha_2 L_2} \approx \frac{2\sqrt{\gamma_1/\tau_R}}{\gamma_2} \gg \frac{\gamma_1}{\gamma_2}, \tag{10}$$

where γ_1 and γ_2 are the total loss rates for the first and second resonators, respectively. Hence, in this limit, the condition for interference becomes $\gamma_1 \ll \gamma_2$, which emphasizes the fact that interference between normal modes requires differential loss in the resonators; i.e., interference does not occur (even though mode splitting occurs) when the loss rates in the two resonators are equal ($\gamma_1=\gamma_2$). Note also that in this limit of small resonator losses, the relative splitting (or distinguishability parameter) varies dramatically for small changes in η, as shown in Fig. 4.

For completeness we note that, in addition to CRIT, coupled-resonator-induced absorption (analogous to electromagnetically induced absorption [12]) can also occur for two-resonator systems, but requires that the resonator farthest from the excitation waveguide be undercoupled—i.e., $a_1 < r_1$. Additionally, an analogy exists between the mode splitting that occurs in CRIT or EIT and the vacuum Rabi splitting that occurs as a result of the underdamped strong coupling between atoms and field modes in an optical cavity [13,14]. Indeed Zhu *et al.* have demonstrated that a simple consideration of the classical linear dispersion of the atoms in the cavity yields a mode splitting equivalent to that predicted by the fully quantum formalism [15]. Vacuum Rabi splitting involves the coupling of the Airy cavity modes with the Lorentzian atomic response and, in this sense, bridges the effects of EIT and CRIT, demonstrating the universality of the mode splitting phenomenon.

The examination of slow light in coupled microresonators [16,17] is simplified by assuming pulse lengths longer than the transient response of the structure, so that each structure is effectively in steady state. This is equivalent to assuming that the input is quasimonochromatic—i.e., that the pulse spectrum is sufficiently narrow in comparison to the CRIT linewidth. The assumption of unidirectional propagation also greatly simplifies the analysis because it enables the coupling between different structures to be ignored. It is also useful to note that the effective phase shift $\tilde{\phi}^{(\mathrm{eff})}$ imparted to light transmitted across a single structure is analogous to the polarizability of a single atom, a two-level atom for the case where the structure consists of a single ring, or a three-level atom in the case where the structure consists of two coupled rings. Therefore, a collection of such structures is analogous to an optical medium, and the contribution to the group index from a single structure within this collection is proportional to $d\tilde{\phi}^{(\mathrm{eff})}/d\phi$. The transformation from "microscopic" to "macroscopic" quantities necessarily involves the density of structures. Hence, ignoring the material dispersion of the waveguide, the relative group index may be written $\delta\tilde{n}=\tilde{n}_g-n=\lambda Z d\tilde{\phi}^{(\mathrm{eff})}/d\phi$, where $\tilde{n}_g$ is the group index, n is the phase index of the waveguide material, $\lambda=1/D$ is the linear number density of structures, $Z=nL=n\pi d$ is the OPL of a single ring, d is the diameter of a single ring, and D is the distance (along the excitation waveguide) between adjacent structures. Hence, the relative group index may be no larger than $(\delta\tilde{n})_{\max}=n\pi d\tilde{\phi}^{(\mathrm{eff})}/d\phi$ for the case where the structures are linearly "close packed"—i.e., when $D=d$. In simple two-level atomic systems, slow (fast) light occurs at the wings (peak) of atomic resonances because the refractive index increases (decreases) rapidly with frequency across the resonance; i.e., normal (anomalous) dispersion occurs. As we have pointed out, in many ways WGM's in microresonators

are analogous to atomic resonances. However, unlike absorption in atomic modes, the loss in microresonators is typically dominated by surface scattering whereas intrinsic absorption is negligible. Radiative (bending) losses can also be significant for sufficiently small resonators. A microresonator may be said to be undercoupled, overcoupled, or critically coupled depending on the coupling-to-loss ratio. On-resonance, single overcoupled resonators ($a_1 > r_1$) result in slow light, whereas single undercoupled resonators ($a_1 < r_1$) result in fast light, and critically coupled resonators ($a_1 = r_1$) result in zero transmission. Undercoupled resonators thus have the same linear dispersion characteristics as atomic resonators—i.e., normal dispersion in the wings and anomalous dispersion at the peak of the resonance. The problem in both single microresonators and two-level atoms is that slow light is accompanied by significant loss, and this is overcome in both cases with the addition of a second resonator coherently coupled to the first, by an external electromagnetic field in the case of EIT or by an intrinsic coupling in the case of CRIT. The effective phase shift $\tilde{\phi}_2^{(\mathrm{eff})}$ and single-structure contribution to the group index $d\tilde{\phi}_2^{(\mathrm{eff})}/d\phi$, are plotted in Figs. 3(b) and 3(c), respectively, for the structure shown in the inset of Fig. 3(a). Strong normal dispersion is observed to accompany the induced transparency for two (or even numbers of) coupled rings, in contrast to the anomalous dispersion (and strong absorption) that occurs for single (or odd numbers of coupled) rings.

As has been pointed out for atoms, larger group delays are associated with smaller EIT linewidths. The same is true for CRIT, and one way to obtain larger dispersion and group delays is simply to use larger resonators. The size of each resonator may be increased by the same amount, or the size of just one of the resonators may be increased such that the OPL of the larger ring is an integer multiple of that of the smaller ring. If, for example, the first resonator is made 4 times larger than the second, such that $\phi_1 = 4\phi_2$, then every fourth resonance of the first ring will be split, and that splitting will be such that the linewidth of the resulting "spectral hole," and hence the group velocity at line center, is 4 times smaller than for the case of equal-sized rings ($\phi_1 = \phi_2$). These effects are observed in Figs. 5(a) and 5(b), where the absorptance A_2 and single-structure group index $d\tilde{\phi}_2^{(\mathrm{eff})}/d\phi_2$ are plotted, respectively, for the case of $a_1 = 0.9999$, $a_2 = 0.88$, $r_1 = 0.999$, $r_2 = 0.9$, and $\phi_1 = 4\phi_2$. This effect is analogous to the case of nondegenerate EIT where the probe frequency is a harmonic of that of the control field.

Moreover, in addition to atomic three-level Λ configurations, EIT is possible in cascade Ξ systems. It has been demonstrated that for n-level cascaded atomic systems, the atomic resonance splits into $n-1$ submodes, as a result of the interference between one- and multiple-photon effects, such that $n-2$ dark states occur in the gaps between the resonances [18]. Hence, EIT occurs on line center when n is odd but is destroyed when n is even. Similarly, for N identical coupled microresonators, the resonance frequency splits into N submodes, as a result of interference between one- and multiple-ring paths. When N is even, a spectral hole appears at the single-ring resonance as a result of CRIT, whereas a peak occurs when N is odd. Thus, because each submode is narrower than the single-ring resonance, the group velocity can be made even smaller when larger numbers of resonators are employed.

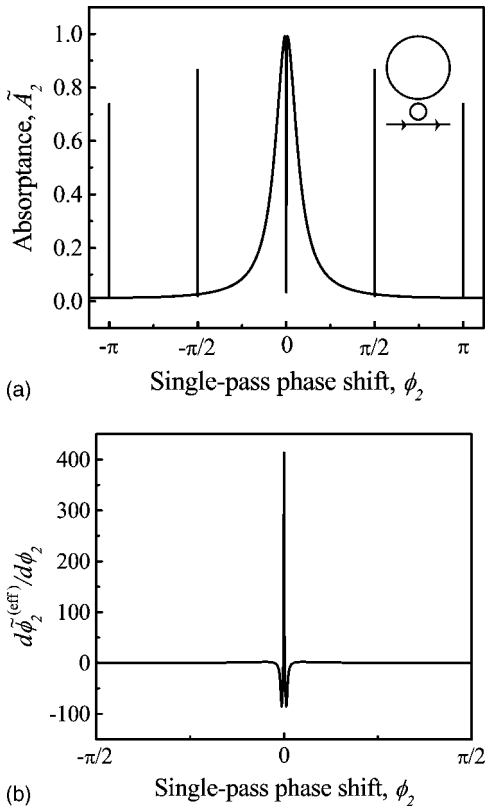

FIG. 5. (a) Absorptance vs single-pass phase shift for two unequal coupled ring resonators such that $\phi_1 = 4\phi_2$, where $a_1 = 0.9999$, $a_2 = 0.88$, $r_1 = 0.999$, and $r_2 = 0.9$. The CRIT linewidth is 4 times smaller than for the case of equal-sized rings ($\phi_1 = \phi_2$). (b) The group index on resonance is 4 times larger than for the case of equal-sized rings ($\phi_1 = \phi_2$).

In summary, we have demonstrated that EIT-like effects can be established in coupled optical resonators due to classical destructive interference. Internal coupling between the resonators is responsible for the splitting, rather than the application of an external control field. Whereas EIT is often limited by absorption of the control field, for CRIT there is no collapse of the splitting with propagation since there is no control field to be absorbed. The CRIT linewidth may be decreased by using larger rings of equal size (analogous to degenerate three-level EIT), by using larger resonators of unequal size where the optical path length of the larger resonator is an integer multiple of that of the smaller one (analogous to nondegenerate three-level EIT), or by using larger numbers of equal-sized resonators (analogous to multilevel EIT). These coupled microresonators can play a role in the implementation of photonic quantum logic gates [19] and offer an alternative approach to quantum well devices [20] for achieving induced transparency in the solid state. A practical difficulty is that CRIT is obscured when the intrinsic loss in the pumping resonator becomes significant, in direct analogy to the condition that $\Gamma_{13} \ll \Gamma$ for the observation of EIT. Even in the absence of CRIT, because the resonance

features are significantly narrower in coupled resonators, the dispersion is much greater, and hence the light is slower (or faster) than in single resonators. However, CRIT has recently been observed in fused silica microspheres [21], which can possess intrinsic quality factors exceeding 10^8, corresponding to attenuation factors $a > 0.9999$. Moreover, in contrast with microfabricated structures, the coupling reflectivity of silica microspheres can be easily adjusted and can approach unity simply by increasing the separation of the spheres.

The work of K. A. Fuller was supported by the NASA Faculty Fellowship Program and by NSF Grant No. ATM-0220465. A.T.R. acknowledges support from a NASA EPSCoR Research Initiation Grant and NSF Grant No. ECS-0115442. R.W.B. acknowledges support from ONR Grant No. N00014-02-1-0797. The authors also acknowledge the Education Programs Office, Technology Investment Program, and Center Director's Discretionary Fund at NASA's Marshall Space Flight Center.

[1] S. E. Harris, Phys. Rev. Lett. **77**, 5357 (1996).
[2] A. G. Litvak and M. D. Tokman, Phys. Rev. Lett. **88**, 95003 (2002).
[3] W. E. Lamb and R. C. Retherford, Phys. Rev. **81**, 222 (1951).
[4] P. R. Hemmer and M. G. Prentiss, J. Opt. Soc. Am. B **5**, 1613 (1988).
[5] G. L. Garrido Alzar, M. A. G. Martinez, and P. Nussenzveig, Am. J. Phys. **70**, 37 (2001).
[6] A. Yariv, Y. Xu, R. K. Lee, and A. Scherer, Opt. Lett. **24**, 711 (1999).
[7] D. D. Smith, H. Chang, and K. A. Fuller, J. Opt. Soc. Am. B **20**, 1967 (2003).
[8] S. H. Autler and C. H. Townes, Phys. Rev. **100**, 703 (1955).
[9] U. Fano, Phys. Rev. **124**, 1866 (1961); U. Fano and J. W. Cooper, *ibid.* **137**, A1364 (1965).
[10] Y. Li and M. Xiao, Phys. Rev. A **51**, 4959 (1995).
[11] G. S. Agarwal, Phys. Rev. A **55**, 2467 (1997).
[12] A. M. Akulshin, S. Barreiro, and A. Lezama, Phys. Rev. A **57**, 2996 (1998).
[13] J. J. Sanchez-Mondragon, N. B. Narozhny, and J. H. Eberly, Phys. Rev. Lett. **51**, 550 (1983).
[14] M. G. Raizen, R. J. Thompson, R. J. Brecha, H. J. Kimble, and H. J. Carmichael, Phys. Rev. Lett. **63**, 240 (1989).
[15] Y. Zhu, D. J. Gauthier, S. E. Morin, Q. Wu, H. J. Carmichael, and T. W. Mossberg, Phys. Rev. Lett. **64**, 2499 (1990).
[16] J. E. Heebner and R. W. Boyd, J. Mod. Opt. **49**, 2629 (2002).
[17] R. W. Boyd and D. J. Gauthier, in *Progress in Optics XXXXIII*, edited by E. Wolf (Elsevier, Amsterdam, 2002).
[18] D. McGloin, D. J. Fulton, and M. H. Dunn, Opt. Commun. **190**, 221 (2001).
[19] T. Opatrny and D. G. Welsch, Phys. Rev. A **64**, 023805 (2001).
[20] G. B. Serapiglia, E. Paspalakis, C. Sirtori, K. L. Vodopyanov, and C. C. Phillips, Phys. Rev. Lett. **84**, 1019 (2000).
[21] A. Naweed and A. T. Rosenberger (private communication).